

# On-Chip Molecular Communication: Analysis and Design

Nariman Farsad, Andrew W. Eckford, Satoshi Hiyama and Yuki Moritani

**Abstract**—We consider a confined space molecular communication system, where molecules or information carrying particles are used to transfer information on a microfluidic chip. Considering that information-carrying particles can follow two main propagation schemes: passive transport, and active transport, it is not clear which achieves a better information transmission rate. Motivated by this problem, we compare and analyze both propagation schemes by deriving a set of analytical and mathematical tools to measure the achievable information rates of the on-chip molecular communication systems employing passive to active transport. We also use this toolbox to optimize design parameters such as the shape of the transmission area, to increase the information rate. Furthermore, the effect of separation distance between the transmitter and the receiver on information rate is examined under both propagation schemes, and a guidepost to design an optimal molecular communication setup and protocol is presented.

## I. INTRODUCTION

Over the past decade there has been considerable advancement in the fields of nanotechnology, biotechnology, and microrobotics, where *micro- or nano-scale devices* are designed and engineered to perform specific tasks such as drug delivery. Because of their small scales, a single micro- or nano-device typically performs a very simple and specific task; in order to fulfill more complex tasks, a *micro- or nano-scale network* called *nanonetwork* [1] must be formed, where each node in the network is a micro- or nano-machine. Therefore, communication between multiple micro- or nano-scale devices is essential.

In this paper, we focus on molecular communication [2], in a confined microfluidic channel on a chip device, and study different molecular propagation schemes from an information theoretical perspective. Although molecular communication is present in nature and is used by micro-organisms such as microbes to communicate and detect other micro-organisms, it was only recently that engineering a molecular communication system has been proposed as means of communication in nanonetworks [3]. In this scheme, an engineered micro- or nano-sized transmitter releases small particles such as molecules or lipid vesicles into a microfluidic medium, where

the particles propagate until they arrive at an engineered micro- or nano-sized receiver. The receiver then detects and decodes the information encoded in these particles. For example, the information can be conveyed from the transmitter to the receiver by encoding messages into the timing, identities, number or concentration of particles.

There are two different propagation schemes in molecular communication: passive transport and active transport [2]. In passive transport, the information carrying particles propagate from the transmitter to the receiver by diffusing in the microfluidic medium without using external energy. In active transport, information carrying particles are transported by an external means such as molecular motors or an external device such as a syringe pump. Inside cells, molecular motors such as kinesin use external energy in the form of adenosine triphosphate (ATP) to move over a track made of microtubules while carrying cargoes, similar to a cargo train. However, typically in molecular communication, as proposed in [4], a microtubule filament moves over a track of molecular motors while carrying a cargo of information particles.

In biology, molecular communication can be employed over short-range (nm scale) communication, mid-range ( $\mu\text{m}$  to cm scale) communication, or long-range (cm to m scale) communication [5], [6]. For example, neurotransmitters use passive transport (free diffusion) to communicate over short-range; inside cells motor proteins are used to actively transport cargoes over the mid-range; and hormones are transported over the long-range using active transport with external power source (flow of blood from the heart). In this work, we consider the mid-range molecular communication because it is the range of interest for lab-on-chip devices with numerous potential applications such as diagnostic chips for healthcare.

There is an emerging body of literature examining molecular communication from an engineering perspective. One aspect of this literature explores the various nanotechnological and biological techniques that can be exploited in order to create a communication system, such as intercellular calcium propagation through gap junctions [7], [8] and molecular propagation mediated by molecular motors [9], [10]. (The reader is directed to [2] for a thorough survey of molecular communication techniques.)

Another aspect of the literature explores molecular communication as a communication system, i.e., from a communication-theoretic and information-theoretic perspective. Notable works in this direction include a general formulation of molecular communication as a timing channel under Brownian motion [11], [12], an analysis of information transfer rates using molecular motors [13], [14], mathemat-

Material in this paper was presented in part at the IEEE International Conference on Nanotechnology, Seoul, South Korea, July 2010, and at the 5th International ICST Conference on Bio-Inspired Models of Network, Information, and Computing Systems, Boston, MA, USA, December 2010.

Nariman Farsad and Andrew W. Eckford are with the Department of Computer Science and Engineering, York University, 4700 Keele Street, Toronto, Ontario, Canada M3J 1P3. Emails: nariman@cse.yorku.ca, aeckford@yorku.ca

Satoshi Hiyama and Yuki Moritani are with Research Laboratories, NTT DOCOMO Inc., Yokosuka, Kanagawa, Japan. Emails: hiyama@nttdocomo.co.jp, moritani@nttdocomo.co.jp

ical channel models for continuous diffusion [15], binary concentration-encoded molecular communication [16], and comparison of achievable information rates under different propagation schemes [17], [18], mathematical modelling of achievable information rates [19], and optimization of the transmission zone and vesicular encapsulation [20]. Notable works concerning molecular motor based active transport molecular communication includes design of molecular sorters and rectifiers [21], [22], a simple mathematical transport model for active transport propagation [19], optimization of the transmission zone and vesicular encapsulation [20], and design and optimization of the channel [23].

In this paper we continue our work from [17]–[19], and study the achievable information transmission rates, in confined microfluidic channels, under different propagation schemes namely, passive transport or Brownian motion, active transport using molecular motors, and active transport using an external device such as a syringe pump. We assume the transmitter and the receiver are perfect (i.e. the transmitter and receiver send and detect particles perfectly without any errors) and only focus on the theoretical achievable information rate of each propagation scheme. In other words, we study which propagation scheme can transmit at a higher rate. Our contributions are as follows:

- We obtain achievable information rates for molecular communication over a confined microfluidic channel based on different propagation schemes, namely Brownian motion and molecular motor based active transport.
- To improve the achievable information rate of simple Brownian motion, we propose the introduction of flow into the microchannel. However, introducing flow would require an external device such as a syringe pump, and therefore passive transport of simple Brownian motion is converted into active transport using an external device.
- We provide a design and analysis tool to improve the information transmission rate of molecular motor based active transport. We use this tool to optimize the design of the transmission area for molecular motor based active transport. We conclude that this optimal transmission area is along the walls of the microchannel since microtubules mostly move along the walls. We also propose further improvements through increasing the number of microtubules.
- As time per channel use increases, although there will be more information particles delivered to the receiver, the channel capacity in bits per second also changes, regardless of the propagation scheme. We show that for a given microchannel and propagation scheme there exists an optimal time per channel use which can be estimated using our analysis toolbox.
- We study the effects of channel size (the separation distance between the transmitter and the receiver) on the information rate under different propagation schemes. We conclude that both molecular motor based active transport and Brownian motion with flow (active transport using an external device) achieve higher information rates compared to simple Brownian motion (passive transport). We

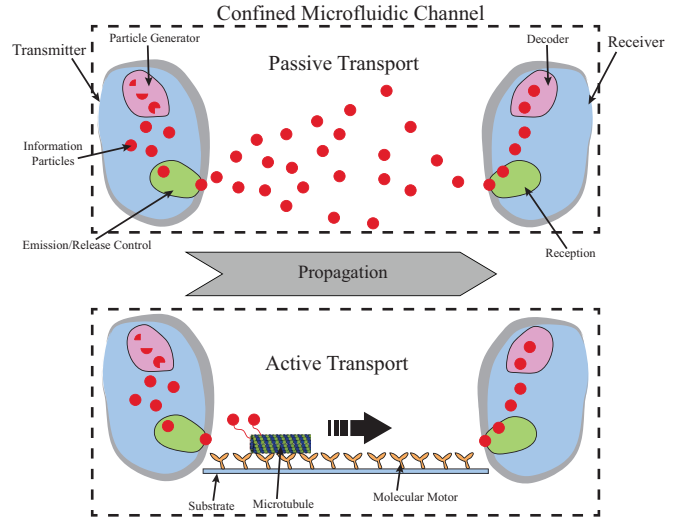


Fig. 1: Two molecular communication systems depicting the transmitters, receivers, the confined microfluidic channel (dashed lines), and different propagation schemes. *TOP*: Passive transport is employed, where the information carrying molecules diffuse in the confined microfluidic environment and follow a Brownian motion path from the transmitter to the receiver. *BOTTOM*: Active transport using stationary molecular motors attached to a glass substrate and microtubules is employed to carry the information particles from the transmitter to the receiver.

also show that for smaller values of time per channel use and smaller separation distances between the transmitter and the receiver, Brownian motion with flow achieves a higher information rate. Moreover we show that for larger values of time per channel use and larger channel dimensions, optimal molecular motor based active transport achieves a higher information rate. However, introducing flow would require an external device such as a syringe pump and is not as straightforward as molecular motor based active transport. Therefore, despite the slight improvement in channel capacity, we conclude that molecular motor based active transport are a more suitable propagation scheme for lab-on-chip applications.

## II. MOLECULAR COMMUNICATION AND ACHIEVABLE INFORMATION RATES

### A. Overview of Molecular Communication

In molecular communication as proposed in [2], [3], a transmitter generates information carrying particles such as molecules or lipid vesicles, and then releases them for transmission to the receiver, over an aqueous environment. Therefore, the transmitter consists of a particle generation module where the information particles are generated, and a release mechanism which oversees the timing, the number, and the type of the particles released. Together particle generation and release modules can encode information into the information carrying particles. For example, the information can be encoded in the release time, type, number, or the concentration

of the particles released. Using this scheme, the particle generation and release mechanisms can be treated as separate problems. Similarly, at the receiver the information particles are captured by a reception module and then decoded using a decoder module in a layered approach.

In this layered approach, the particles propagate inside a confined microfluidic channel, between the transmitter's release module and the receiver's reception module, as shown in Figure 1. There are three major propagation schemes: passive transport, active transport using molecular motors, and active transport using an external device such as a syringe pump. When passive transport is employed, the particles diffuse in the fluidic environment and follow a random Brownian motion until they arrive at the receiver. When active transport using molecular motors is employed, a molecular motor system consisting of kinesin and microtubule filaments can be used to transport the particles from the transmitter to the receiver. In active transport using an external device, a syringe pump is used to create a flow that would assist the simple Brownian motion of the information particles. In this paper we sometimes refer to this type of active transport as *Brownian motion with flow*.

In active transport using a molecular motors, a loading and an unloading mechanism for picking up information particles from the transmitter and dropping off the particles at the receiver is necessary. In [4], [24], single stranded deoxyribonucleic acids (ssDNA) and the corresponding hybridization bonds between complementary ssDNA pairs is proposed for the loading and the unloading mechanisms. Microtubules moving over a kinesin covered glass substrate are covered with 15 base ssDNAs, and the information particles are also covered with 23 base ssDNAs which is complementary to that of the microtubules' ssDNAs. When the microtubule glides close to an information particle, the two ssDNA sequences hybridize and the microtubule carries the information particle until it gets close to the receiver. The receptor module at the receiver is covered with 23 base ssDNAs, which are complementary to that of the information particles. When a loaded microtubule filament glides close to the receptor module, it will unload the information particle through hybridization bound with the complementary 23 base ssDNA at the receptor module. Since 23 base hybridization bound is stronger than the 15 base hybridization bound between the particles and the microtubules, the particles are unloaded at the receiver.

Although these propagation schemes are stochastic, it is not clear which performs better and can achieve a higher information transmission rate. Brownian motion is more "random" than the microtubule's motion over a kinesin covered glass substrate. However in Brownian motion, information particles start propagating as soon as they are released into the fluidic channel by the release control module at the transmitter, while in molecular motor based active transport they remain at the release control module until they are picked up by the microtubules. Furthermore, it is unclear how the shape of the transmitter, receiver, and the confined microfluidic channel effects the information rate. Moreover, if the shape of these components effects the information rate, it is not clear if there exists an optimal shape that would maximize the information

rate.

In this work, we study the channel capacity (maximum achievable information rate) of different propagation schemes. Because of the layered approach presented in Figure 1, we can focus on the propagation scheme regardless of the transmitter and the receiver design. In the rest of this paper, we assume the transmitter and the receiver are perfect and can encode, release, receive, and decode the information carrying particles flawlessly.

## B. Information Theory and Achievable Information Rate

Previous work has considered molecular communication either as a *timing channel* problem (i.e., where information is encoded in the times when molecules are released) [11], [13]; as an *inscribed matter* problem (i.e., where information is encoded by transmitting custom-made particles, such as specific strands of DNA) [25]; or as a *mass transfer* problem (i.e., a message is transmitted by moving a number of particles from the transmitter to the receiver) [16]–[18].

In this paper, we consider information transmission as a mass transfer problem. In the simplest possible conception of this scheme, the particles themselves are not information-bearing, and a message is conveyed in the *number* of particles released by the transmitter. For example, if a maximum of three particles may be used, from a traditional communication system perspective, we may form messages two bits long (i.e.,  $\log_2 4$ ): "00" for 0 particle, "01" for 1 particle, "10" for 2 particles, and "11" for 3 particles. However, this message might not be perfectly conveyed to the receiver: given a time limit  $T$  for the communication session, it is possible that some of the particles will not arrive at the receiver after  $T$  has elapsed. We refer to time limit  $T$  as *time per channel use*. In other words, time per channel use is a predefined amount of time representing the time duration for a single message transmission session, and it is one of the parameters of the molecular communication system.

Let  $\mathcal{X} = \{0, 1, 2, \dots, x_{max}\}$  be the set of possible transmission symbols,  $x_{max}$  be the maximum number of particles the transmitter can release per channel use, and  $X \in \mathcal{X}$  be the number of information particles released into the medium by the transmitter. In a traditional communication system, the received symbols at the receiver are corrupted with noise from the environment, while in the molecular communication system, the received symbols are corrupted because of the random propagation of particles. Let  $Y \in \mathcal{X}$  represent the number that arrive at the destination after time per channel use  $T$ . From the channel's perspective,  $X \in \mathcal{X}$  is a discrete random variable given by probability mass function (PMF)  $f_X(x)$ , and  $Y \in \mathcal{X}$  is also a discrete random variable given by PMF  $f_Y(y)$ ,

The maximum rate at which any communication system can *reliably transmit information* over a noisy channel is bounded by a limit called *channel capacity* [26]. The channel capacity can be calculated as,

$$C = \max_{f_X(x)} I(X; Y), \quad (1)$$

where  $I(X; Y)$  is the mutual information between  $X$  and  $Y$ . Mutual information is defined as

$$I(X; Y) = E \left[ \log_2 \frac{f_{Y|X}(y|x)}{\sum_x f_{Y|X}(y|x) f_X(x)} \right], \quad (2)$$

where,  $f_{Y|X}(y|x)$  represents the probability of receiving symbol  $y$  at the destination, given that symbol  $x$  was transmitted by the source;  $f_X(x)$  represents the probability of transmitting symbol  $x$ ; and  $E[\cdot]$  represents expectation.

Clearly, there exists some PMF  $f_{Y|X}(y|x)$  of the number of arrived particles given the number of transmitted particles. If this PMF is known, we can calculate mutual information for any  $f_X(x)$ . However, in order to calculate the channel capacity we need to find the PMF  $f_X(x)$  that maximizes mutual information. We can use the Blahut-Arimoto algorithm [27], [28] to find the PMF  $f_X(x)$  such that, given  $f_{Y|X}(y|x)$ , mutual information is maximized. Therefore, if PMF  $f_{Y|X}(y|x)$  is known, we can calculate the channel capacity of the molecular communication system in a straightforward manner.

Finding the PMF  $f_{Y|X}(y|x)$  is non-trivial because of the shape and the geometry of the molecular communication channels, which generally rule out closed-form solutions. For example, mathematically it is well known that Brownian motion can be described by stochastic differential equations, and properties of the motion (such as first arrival time distributions) can be derived from solutions of these equations. However, in confined spaces, solutions are generally not available in closed form. To overcome this issue, the PMF can be estimated using Monte Carlo simulations. In order to do this, we first create a computer simulation environment where the actual random motion of the particles, for both Brownian motion and molecular motor based active transport, is modelled. Then, we simulate this propagation from a hypothetical transmitter to a hypothetical receiver many times until a good estimate of the PMF  $f_{Y|X}(y|x)$  can be obtained. Using this estimate, we then calculate the channel capacity and therefore, the maximum achievable information rate. In the next section, we describe this simulation environment.

### III. SIMULATION ENVIRONMENT AND MODELLING PROPAGATION

Our molecular communication setup shown in Figure 2 is a rectangular propagation environment (with negligibly rounded corners to help make our simulation software faster), representing a channel on a microfluidic chip, with a fixed width and height of  $20\mu\text{m}$  and  $10\mu\text{m}$ , consisting of a *transmission zone* on the left and a *receiver zone* on the right. Please note, Figure 2 is the top view of the simulation environment and does not show the height of the channel. Regardless of the propagation model, message-bearing vesicles originate at the transmission zone, and propagate until they arrive at the receiver zone. The separation between the transmission zone and the receiver zone and hence the length of the environment is variable with different separation values of  $20\mu\text{m}$ ,  $40\mu\text{m}$  and  $60\mu\text{m}$ . In the rest of this paper, we consider this particular setup and use it as the basis for our simulation and comparison of different propagation schemes.

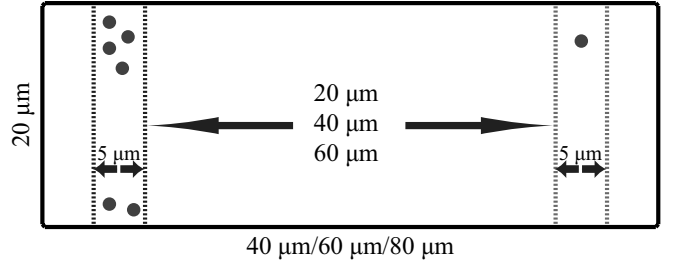


Fig. 2: Depiction of the simulation environment. In this figure, dots represent information particles. The transmission zone is on the left (darker dashed strip), and the receiver is on the right (lighter dashed strip). The width of the channel is constant at  $20\mu\text{m}$ . The height of the channel, not shown here, is also constant at  $10\mu\text{m}$ . The distance between the transmission area and the receiver area and hence the length of the channel is variable.

#### A. Simulating Brownian Motion

Brownian motion refers to the random motion of a particle as it collides with other molecules in its vicinity. Through this random motion the information carrying particles propagate from the transmission zone to the receiver zone. Following [29], we perform *Monte Carlo* simulations on particles in order to obtain the needed properties of the motion. In particular, we perform a three-dimensional discrete-time simulation of information carrying particles, for  $\Delta t$  time intervals. Given some initial position  $(x_0, y_0, z_0)$  at time  $t = 0$ , for any integer  $k > 0$ , the motion of the particles is given by the sequence of coordinates  $(x_i, y_i, z_i)$  for  $i = 1, 2, \dots, k$ . Each coordinate  $(x_i, y_i, z_i)$  represents the position of the particle at the end of time  $t = i\Delta t$ , where

$$x_i = x_{i-1} + \Delta r \cos \theta_i \cos \phi_i, \quad (3)$$

$$y_i = y_{i-1} + \Delta r \sin \theta_i \cos \phi_i, \quad (4)$$

$$z_i = z_{i-1} + \Delta r \sin \phi_i, \quad (5)$$

where  $\Delta r$  is the particle's displacement over each time interval of  $\Delta t$ , and both  $\theta_i$  and  $\phi_i$  define the angle of displacement in 3-dimensional space over the time interval  $\Delta t$ . Furthermore, Over each time interval of  $\Delta t$ , the particle's displacement  $\Delta r$  is given by

$$\Delta r = \sqrt{4D\Delta t}, \quad (6)$$

where  $D$  is the free diffusion coefficient. For a given particle and fluid propagation environment,  $D$  is given by

$$D = \frac{k_B T}{6\pi\eta R_H}, \quad (7)$$

where  $k_B = 1.38 \cdot 10^{-23}$  J/K is the Boltzman constant,  $T$  is the temperature (in K),  $\eta$  is the dynamic viscosity of the fluid, and  $R_H$  is the hydraulic radius of the molecule. We assume that  $D$  is the same throughout the medium, and that collisions with the boundaries are elastic. Moreover, we assume particles do not get stuck to the walls. In [29], values of  $D$  ranging from  $1-10 \mu\text{m}^2/\text{s}$  were considered realistic for signalling molecules. Finally the angle,  $\theta_i$  is an independent, identically distributed (iid) random variable for all  $i$ , uniformly distributed on  $[0, 2\pi)$ ,

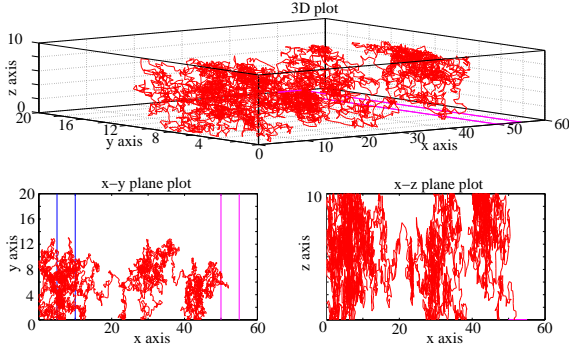


Fig. 3: A sample Brownian movement of a single particle in three dimensions, from the transmitter area to the receiver area.

and the angle  $\phi_i$  is also an iid random variable, uniformly distributed on  $[-\pi/2, \pi/2)$ .

In our simulation we assume that the particles initially start propagating randomly and uniformly on the  $(x, y)$  plane of the transmission zone, but  $z$  is set to the maximum vertical height (i.e., the particles are “dropped” onto the microchannel at the transmission zone). Furthermore, the particles start moving as soon as they are released into the microchannel by the transmitter. The propagation halts as soon as the particle arrives at the receiver zone. The receiver zone is on the bottom right side and it is a box with a small height of 23nm representing the height of the 23 base ssDNAs that are used to capture the information particles.

Using these equations, to calculate the PMF  $f_{Y|X}(y|x)$ , we simulate the Brownian motion of a single particle from the transmitter to the receiver as shown in Figure 3. By repeating these simulation trials we can calculate the probability that a single particle arrives at the destination in  $T$  seconds. Letting  $p_a$  represent this probability, the PMF  $f_{Y|X}(y|x)$  has the binomial distribution, given by

$$f_{Y|X}(y|x) = \begin{cases} \binom{x}{y} p_a^y (1-p_a)^{x-y}, & 0 \leq y \leq x \\ 0, & \text{otherwise} \end{cases} \quad (8)$$

Thus,  $p_a$  is found by simulating many trials of a single particle’s motion over  $T$  seconds, and counting the fraction that arrive. Note that different simulations are necessary for different values of  $T$ . Furthermore, because the motion of each particle is independent of the other particles released by the transmitter,  $f_{Y|X}(y|x)$  has a binomial distribution.

### B. Simulating Molecular Motor Based Active Transport

When active transport using molecular motors is employed, as in Section II-A, we assume that the microchannel is lined with static kinesin motors, which cause microtubule filaments to propagate along their surface, carrying information-bearing particles from the transmitter to the receiver. We also assume that the particles are anchored to the transmission area until they are picked up by the microtubules for delivery to the destination. Therefore, instead of simulating the motion of

particles we must simulate the motion of the microtubules moving over kinesin covered substrate.

The motion of the microtubule is largely regular, although the effects of Brownian motion cause random fluctuations. Again we use Monte Carlo simulations to obtain the needed properties of the motion, using the schemes from [21] and [22]. However, since the microtubules move only in the  $x$ - $y$  directions, and do not move in the  $z$  direction (along the height of the channel), we consider a two-dimensional simulation of microtubules for  $\Delta t$  time intervals. Given some initial position  $(x_0, y_0)$  at time  $t = 0$ , for any integer  $k > 0$ , the motion of the microtubule is given by the sequence of coordinates  $(x_i, y_i)$  for  $i = 1, 2, \dots, k$ . Each coordinate  $(x_i, y_i)$  represents the position of the microtubule’s head at the end of the time  $t = i\Delta t$ , where

$$x_i = x_{i-1} + \Delta r \cos \theta_i, \quad (9)$$

$$y_i = y_{i-1} + \Delta r \sin \theta_i. \quad (10)$$

In this case, the step size  $\Delta r$  at each step is an iid Gaussian random variable with mean and variance

$$E[\Delta r] = v_{\text{avg}} \Delta t, \quad (11)$$

$$\text{Var}[\Delta r] = 2D \Delta t, \quad (12)$$

where  $v_{\text{avg}}$  is the average velocity of the microtubule, and  $D$  is the microtubule’s diffusion coefficient. The angle  $\theta_i$  is no longer independent from step to step: instead, for some step-to-step angular change  $\Delta\theta$ , we have that

$$\theta_i = \Delta\theta + \theta_{i-1}. \quad (13)$$

Now, for each step,  $\Delta\theta$  is an iid Gaussian-distributed random variable with mean and variance

$$E[\Delta\theta] = 0, \quad (14)$$

$$\text{Var}[\Delta\theta] = \frac{v_{\text{avg}} \Delta t}{L_p}, \quad (15)$$

where  $L_p$  is the persistence length of the microtubule’s trajectory. In [21], these values were given as  $v_{\text{avg}} = 0.85 \mu\text{m/s}$ ,  $D = 2.0 \cdot 10^{-3} \mu\text{m}^2/\text{s}$ , and  $L_p = 111 \mu\text{m}$ . Following [21], in case of a collision with a boundary, we assume that the microtubule *does not reflect off the boundary*, as in an elastic collision, but instead sets  $\theta_i$  so as to *follow the boundary*.

The starting location of the microtubule is assumed to be random and uniformly distributed across the entire propagation area. Moreover, the initial directional angle  $\theta_0$  is selected uniformly at random from the range  $[0, 2\pi]$ , and microtubules are assumed to be initially unloaded (without any cargoes). We also assume, as proposed in [4], DNA hybridization bond is used to anchor the information particles to the transmission area. Similarly, ssDNAs on the surface of the microtubules hybridize with the ssDNAs on the surface of the information particles when a microtubule passes in close proximity, thereby loading the particles onto the microtubule. From experimental observations it is evident that microtubules can load multiple information particles [4]. Therefore, the loading of a particle happens only if a microtubule with available cargo spots passes in close proximity of a particle.

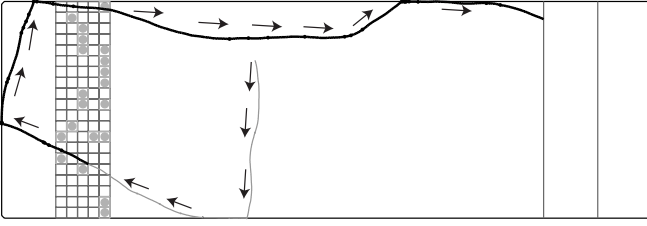


Fig. 4: A sample trajectory of active transport. The microtubule initially starts to the right of the receiver zone (strip on the right side of the microchannel), and moves down and then left (Lighter thinner line). It passes through the transmission zone (grid with empty and particle-bearing tiles) loads a particle at which point the line turns darker and thicker indicating a loaded microtubule. Then the microtubule passes through again, loading another particle (maximum load is assumed to be 5). The loaded microtubule then travels toward the receiver zone, where it delivers the two particles and the trajectory terminates.

In order to capture this loading effect in our simulations, we divide the transmission zone into a square grid, where the length of each square in the grid is the same as the diameter of the information particle. We then distribute particles randomly and uniformly among the squares in the grid. If a microtubule enters a square which is occupied by a particle, and it has an empty cargo slot available, we assume the microtubule loads that particle. In general, we assume that the microtubules can load multiple particles and the maximum number of particles a microtubule can load is given by half of its length divided by the diameter of the particles. This assumption is based on experimental observations. For unloading at the receiver, we assume all the loaded particles are dropped off as soon as a loaded microtubule enters the receiver zone. Figure 4 shows a sample trajectory with the loading and unloading mechanism.

To calculate the PMF  $f_{Y|X}(y|x)$ , for a given number of particles released by the transmitter ( $x$ ), the motion of a microtubule is simulated for  $T$  seconds and the number of particles delivered to the receiver ( $y$ ) is measured at the end of  $T$  seconds. By repeating this process the PMF  $f_{Y|X}(y|x)$  can be estimated for the time duration  $T$ . The whole simulation process can be repeated for different values of  $x$ . Since for each value of  $x$  and  $T$  a set of simulations is necessary, this process can be inefficient. Therefore, in the next subsection we present a mathematical model based on simpler simulations.

### C. Mathematical Model of Molecular Motor Based Active Transport

Assume that our grid transmission zone contains  $n$  squares (i.e. the maximum number of particles that can be anchored to the transmission zone is  $n$ ). As explained before, let  $X \leq n$  be the number of particles at the transmission zone in the beginning, and let  $Y \leq X$  be the number of particles delivered to the receiver zone after time duration  $T$ . Let  $X_i$  be a Bernoulli random variable representing the event where a particle is placed in the  $i$ th square for  $i = 1, 2, \dots, n$ .

Therefore, if we assume that  $X_i$  are independent of each other, the probability that an information particle is placed in the  $i$ th square is given by

$$p(X_i = 1) = \frac{X}{n}, \quad (16)$$

where particles are distributed uniformly among squares. Note that the independence assumption here is an approximation because it does not satisfy the constraint

$$X = \sum_{i=1}^n X_i. \quad (17)$$

Let  $V_i$  be a Bernoulli random variable representing the event that the  $i$ th square is visited by the microtubule in a single trip from the receiver zone, to the transmission zone, and back. Therefore,  $p(V_i = 1)$  represents the probability that the  $i$ th square is visited and  $p(V_i = 0)$  the probability that it is not visited. This probability distribution can quickly be calculated using simple Monte Carlo simulations for any molecular communication channel. For example, the top part of the Figure 5 shows this probability distribution for squares of size  $1\mu\text{m}$  covering the left side of the microchannel. From the probability distribution, it can be seen that the squares close to the walls are visited the most, which is a property of the motion of the microtubules.

Let  $K$  be another random variable representing the number of microtubule trips between the transmission and the receiver zone in time duration  $T$ . The probability distribution for  $K$  is given in [17], and can be quickly calculated for any molecular communication channel using simple Monte Carlo simulations. Let  $V_i^{(k)}$  be a Bernoulli random variable representing the event that the  $i$ th square is visited at least once by the microtubule during  $k$  trips. Therefore,

$$p(V_i^{(k)} = 1) = 1 - (1 - p(V_i = 1))^k, \quad (18)$$

represents the corresponding probability distribution.

Let  $D_i^k$  be a Bernoulli random variable representing the event that a particle from the  $i$ th square is delivered to the destination after  $k$  trips. Then, the probability distribution of  $D_i^k$  is given by

$$p(D_i^{(k)} = 1) = p(V_i^{(k)} = 1)p(X_i = 1), \quad (19)$$

assuming  $p(V_i^{(k)} = 1)$  and  $p(X_i = 1)$  are independent. This independence assumption is not accurate since  $p(X_i = 1)$  changes depending on the number of particles already delivered in previous trips. In general this assumption becomes less accurate as the number of trips  $k$  increases or in other words the channel time duration  $T$  increases. Let  $Y^{(k)}$  be the total number of particles delivered to the receiver zone during  $k$  trips. Then,  $Y^{(k)}$  is given by

$$Y^{(k)} = \min\left(\sum_{i=1}^n D_i^k, X\right), \quad (20)$$

for any given  $X$ . Since  $\sum_{i=1}^n D_i^k$  represents a Poisson-Binomial distribution, its corresponding probability distribution can be calculated using [30]. Finally, we can calculate

PMF  $f_{Y|X}(Y|X)$  as

$$f_{Y|X}(Y|X) = \sum_{k \in K} p(Y^{(k)} | X)p(k), \quad (21)$$

where  $p(Y^{(k)} | X)$  is the probability mass function of  $Y^{(k)}$  given in Equation (20), and  $p(k)$  is the probability mass function of  $K$ , the number of trips between the transmitter and receiver during the time duration  $T$ .

The benefits of this model is twofold. First, it can be employed to quickly estimate the information rate of any molecular communication system, and although it relies on simulations for calculating the probability distributions of  $V_i$  and  $K$ , these simulations are very simple and can be performed on an average computer quickly compared to the Monte Carlo simulation presented in the previous section. Second, because of the model's simplicity, various design problems can be solved, for example, in the next section we use this model to generate an optimal transmission zone. The only drawback of this model is that the resulting PMF,  $f_{Y|X}(Y|X)$ , is not as accurate as the one derived using Monte Carlo simulation scheme used in [18].

#### IV. IMPROVING INFORMATION RATE

In the previous section, we described a simple molecular communication system employing either active transport using molecular motors or passive transport using Brownian motion. We also presented simulation schemes for calculating the channel capacity based on each propagation technique. In this section, we propose a number of methods for further improving the channel capacity.

##### A. Brownian Motion with Flow

In general, we can improve the channel capacity if we transfer information particles from the transmitter to the receiver quicker on average. In Brownian motion, one way to achieve this task is by introducing flow in the direction of transmitter to the receiver. However, Brownian motion with flow requires an external device such as a syringe pump to produce the flow. Therefore, by introducing flow the passive transport of simple Brownian motion is converted into active transport using an external device. Compared to active transport using molecular motors, introducing flow at small scales is not easy and would require a lot of energy with respect to the size of the system.

In its simplest form, introducing flow will change Equations (3)-(5) into,

$$x_i = x_{i-1} + v_{F_x} \Delta t + \Delta r \cos \theta_i \cos \phi_i, \quad (22)$$

$$y_i = y_{i-1} + v_{F_y} \Delta t + \Delta r \sin \theta_i \cos \phi_i, \quad (23)$$

$$z_i = z_{i-1} + v_{F_z} \Delta t + \Delta r \sin \phi_i, \quad (24)$$

where  $v_{F_x}$ ,  $v_{F_y}$ , and  $v_{F_z}$  are flow velocities in the  $x$ ,  $y$ , and  $z$  directions [29]. In this work, the flow velocities are assumed to be constant throughout the molecular communication channel. Although this assumption is not realistic, it provides an idea of the possible gains.

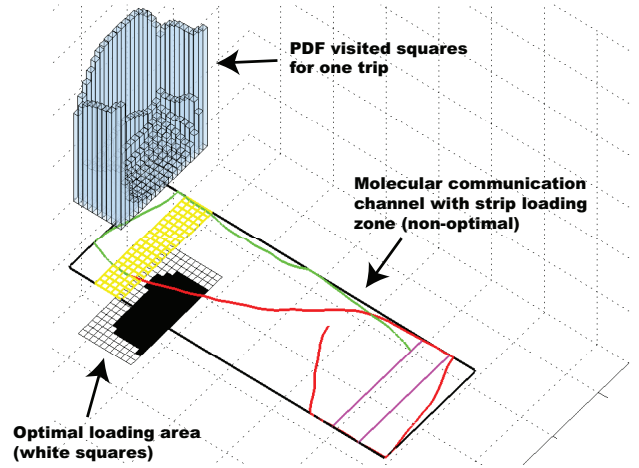


Fig. 5: (Top): Probability distribution of  $p(V_i = 1)$  for squares of size  $1\mu\text{m}$  to the left side of the transmission area. (Middle): Strip transmission area for  $n = 100$  squares. (Bottom): Projection of the probability distribution  $p(V_i = 1)$  on top. The 100 highest values of  $p(V_i = 1)$  are shown in as white squares and they represent the optimal transmission area.

##### B. Improving Molecular Motor Based Active Transport

Again, we can improve channel capacity if we transfer information particles from the transmitter to the receiver quicker on average. We propose two possible schemes: increasing the number of microtubules and optimizing the transmission zone.

In the first scheme, by increasing the number of microtubules, more information particles could be picked up and transported to the receiver area during time duration  $T$ . From experimental results, it is evident that microtubules generally move independently of each other, and therefore we make the same assumption in our simulations, when employing multiple microtubules.

In the second scheme, we use our mathematical model presented in Section III-C, and the fact that the microtubules mostly move along the walls of the molecular communication channel, to optimize the transmission area. Consider the top part of Figure 5, illustrating that  $p(V_i = 1)$  (probability that a square is visited in one microtubule trip) is higher for squares close to the walls of the molecular communication channel. An information particle is picked up from the transmission zone, and delivered to the receiver zone, if the corresponding square is visited. Therefore, we want to find squares with maximum  $p(V_i = 1)$ , which are squares that have the highest probability of being visited during one trip. If information particles are placed there, they have the highest probability of being loaded and therefore of being delivered. In the top part of Figure 5, we plot the probability distribution of all the squares of length  $1\mu\text{m}$  to the left of transmission area (the bar plot). In the middle part, our original strip transmission area (Figure 4) with 100 squares is presented. The bottom plot shows the projection of the probability distribution function of  $p(V_i = 1)$ . The first 100 squares with highest probabilities are shown as white squares, and the rest of the squares are shown

in black. In this projection, the minimum distance between the transmission area and the receiver area is similar to that of the strip transmission area and we have not moved the transmission and receiver physically closer. Finally, according to our mathematical model, this white area is the optimal transmission zone that will give us the highest information rate because probability of visiting and picking up particles is highest.

Unlike the improvement technique proposed for Brownian motion (i.e. flow), these improvements are internal to the molecular communication system and do not require any external device or extensive use of energy.

## V. RESULTS

In this section we present our simulation results, for the molecular communication system proposed in Section III, with variable separation distance between the transmitter and the receiver, employing different propagation schemes.

When Brownian motion is used for propagation, we use the following simulation parameters: simulation time steps of  $\Delta T = 0.1$  seconds, and the free diffusion coefficient  $D = 1 \mu\text{m}^2/\text{s}$ . Therefore, from Equation 6, at each simulated time step the information particles moves  $\Delta r = \sqrt{0.4} \mu\text{m}$  in a random directions. The same values are also used when Brownian motion with flow is considered. The flow is assumed to be always in the direction from the transmitter to the receiver (i.e. the flow velocities in the  $y$  and  $z$  direction are zero and positive in the  $x$  direction.)

For simulating the motion of the microtubule, when molecular motor based active transport is employed, we use the following parameters: simulation time steps of  $\Delta T = 0.1$  seconds, microtubule diffusion coefficient  $D = 2.0 \cdot 10^{-3} \mu\text{m}^2/\text{s}$ , average speed of the microtubule  $v_{\text{avg}} = 0.5 \mu\text{m}/\text{s}$ , and persistence length of the microtubules trajectory  $L_p = 111 \mu\text{m}$ . We also assume the size of the information particles is  $1 \mu\text{m}$ , the average length of the microtubules is  $10 \mu\text{m}$ , and each microtubule can load up to 5 information particles in one trip from the transmission zone to the receiver zone. These parameters are all selected based on experimental observations of ssDNA covered microtubules moving over a kinesin covered substrate.

We assume the set of possible transmission symbols are  $\mathcal{X} = \{0, 1, 2, \dots, x_{\text{max}}\}$ , for some value of  $x_{\text{max}}$ , where a transmission symbol  $X \in \mathcal{X}$  is represented by release of  $X$  information particles into the medium. In the case of active transport using molecular motors, all the released particles will be randomly distributed and will remain stationary at the transmission zone until they are picked up for delivery by a microtubule. By simulating the motion of the particles or the motion of the microtubules many times, we estimate the PMF  $f_{Y|X}(y|x)$  under each propagation scheme. We then use Blahut-Arimoto algorithm [27], [28] to find the PMF  $f_X(x)$ , that would maximize the mutual information, and hence calculate the channel capacity for each propagation scheme.

### A. Brownian Motion Versus Molecular Motor Based Active Transport

First, we compare simple Brownian motion (passive transport), Brownian motion with flow (active transport using an external device), and molecular motor based active transport over a constant channel dimensions. For this set of simulations we use a channel length of  $60 \mu\text{m}$  which results in a  $40 \mu\text{m}$  separation between the transmitter and the receiver. For Brownian motion with flow, flow values of 0.2 and 0.3  $\mu\text{m}/\text{s}$  are considered, while for active transport using molecular motors, 1 and 15 microtubules as well as the strip and optimal transmission area are considered.

Figure 6a, shows the channel capacity in bits versus the maximum possible number of transmission particles ( $x_{\text{max}}$ ), for the time duration of 1000 seconds per single channel use. The value of 1000 seconds is presented since the plots are easily distinguishable for this time duration. From the graph we can see that as we increase the transmission symbol set, the channel capacity increases for all propagation schemes. Also Brownian motion with flow achieves a much higher information rate than simple Brownian motion without flow, and the optimal molecular motor based active transport with 15 microtubules and optimal transmission zone has a much higher channel capacity compared to the non-optimal one (a single microtubule and strip loading area).

From Figure 6a we can see that simple Brownian motion has the lowest channel capacity even slightly lower than molecular motor based active transport using a single microtubule and strip transmission area. Molecular motor based active transport with the optimal transmission area and multiple microtubules achieves the highest channel capacity. Furthermore, flow value of  $0.2 \mu\text{m}/\text{s}$  achieves a higher channel capacity compared to flow value of  $0.3 \mu\text{m}/\text{s}$  since the receiver area is  $5 \mu\text{m}$  away from the back wall as shown in Figure 2. Therefore, because we assume the transmission area is on top and the receiver area is on the bottom, the higher flow values cause the information particles to pass over the receiver zone and be pinned against the back wall. As the result it would take the information particles longer to arrive at the receiver.

The channel capacity in bits per seconds versus the value of time per single channel use is presented in Figure 6b. Different values of time duration per single channel use are considered, ranging from 50 seconds to 2000 seconds. The transmission symbol set is fixed at  $\mathcal{X} = \{0, 1, 2, \dots, 40\}$ . The channel capacity in bits per seconds is then calculated by dividing the capacity in bits with the corresponding time duration per single channel use,  $T$ . As we can see from the graph the channel capacity initially increases as the  $T$  increases, reaches a peak, and then start to decrease. This peak value represents the optimal value of time per single channel use  $T$ .

Again we can see that simple Brownian motion has the lowest channel capacity (i.e peak value), even lower than unoptimized molecular motor based active transport using a single microtubule. However, Brownian motion with  $0.3 \mu\text{m}/\text{s}$  flow achieves the highest channel capacity. Similarly, in the case of the molecular motor based active transport, increasing the number of microtubules, and using the optimal transmission

area, will increase the peak values and shifts the peak location to lower  $T$  values.

### B. Effects of Separation Distance

In these simulations we change the separation between the transmitter and the receiver to see the effects on each propagation scheme. Since we have shown that Brownian motion with flow (active transport using an external device) and molecular motor based active transport using multiple microtubules with optimal transmission area achieve better information rates, we only consider these schemes in our comparison.

In Figure 7a, the channel capacity versus  $x_{max}$  is considered for separation distances of  $20\mu\text{m}$  (red plots),  $40\mu\text{m}$  (blue plots) and  $60\mu\text{m}$  (green plots). The time per channel use is fixed at 750 seconds since the plots are more easily distinguishable at this duration. We can see that regardless of the separation distance molecular motor based active transport with optimal transmission zone and 15 microtubules achieves higher channel capacity. Also for a given propagation scheme, as the separation distance increases channel capacity decreases.

The channel capacity in bits per seconds versus time per single channel use is presented in Figure 7b. Different values of time duration per single channel use are considered, ranging from 50 seconds to 2000 seconds. The transmission symbol set is fixed at  $\mathcal{X} = \{0, 1, 2, \dots, 40\}$ . In general, we see that regardless of the propagation scheme, as the separation distance increases the information rate decreases. We can also see that for separation distance of  $20\mu\text{m}$  (red plots), Brownian motion with flow reaches a higher peak than molecular motor based active transport. However as the separation distance is increased to  $60\mu\text{m}$  (green plots), the difference between the peaks lessens with active transport using molecular motors achieves a slightly higher information rate.

Although we conclude that Brownian motion with flow is slightly better at smaller separation distances, while optimized molecular motor based active transport is slightly better at larger distances, introducing flow would require an external device such as a syringe pump and is not as straightforward as molecular motor based active transport. Therefore, we believe that molecular motor based active transport are a more suitable choice for lab-on-chip applications.

## VI. DISCUSSION, CONCLUSION, AND FUTURE WORK

In this work, we considered a confined space molecular communication system employing different propagation methods. In particular we considered Brownian motion (passive transport), Brownian motion with flow (active transport using an external device), and molecular motor based active transport propagation schemes. We also proposed an encoding scheme based on the number of information particles released by the transmitter, and discussed the calculation of the channel capacity under the proposed propagations. Since this calculation is nontrivial, a simulation toolbox for estimation of channel capacity based on Monte Carlo techniques is developed.

Various techniques for improving the channel capacity of simple Brownian motion and molecular motor based propagation scheme are discussed. Introducing flow is proposed as

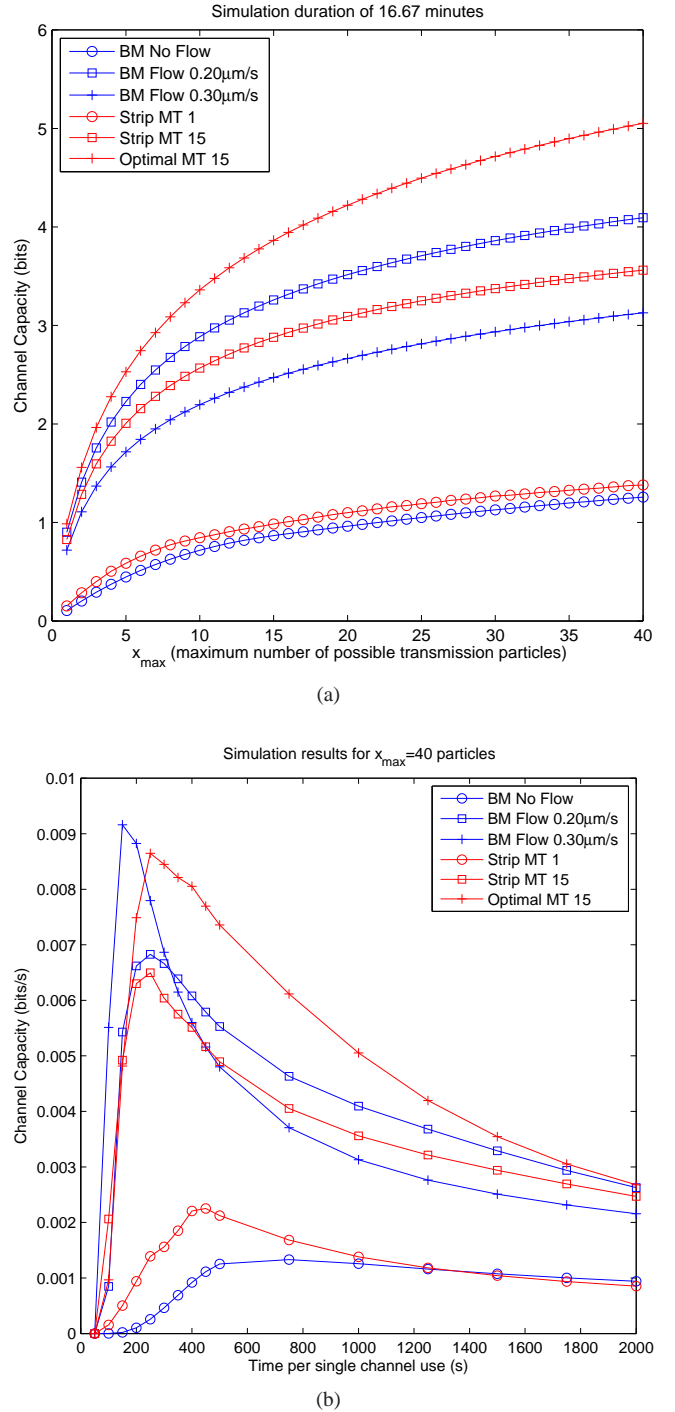
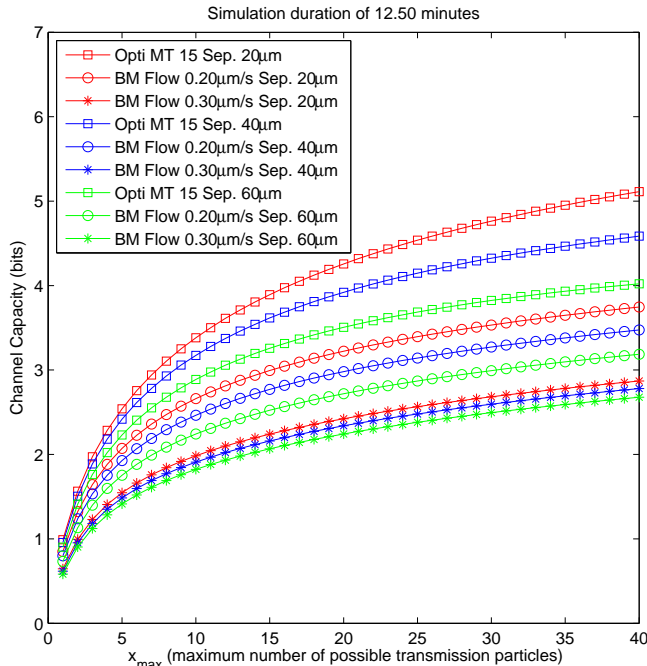
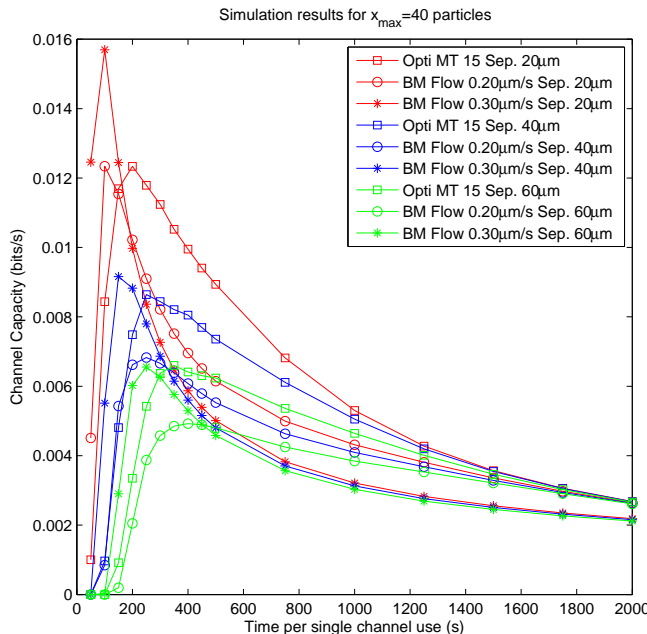


Fig. 6: (a) Channel capacity in bits versus the maximum number of possible transmission particles for Brownian motion (with and without flow) and molecular motor based active transport. Time per channel use is 1000 s. (b) Channel capacity in bits per seconds versus time per channel use for Brownian motion (with and without flow) and molecular motor based active transport. ( $x_{max} = 40$ ).



(a)



(b)

Fig. 7: (a) Channel capacity in bits versus the maximum number of possible transmission particles for Brownian motion with flow and molecular motor based active transport. Time per channel use is 750 seconds and different separations between the transmitter and receiver are considered. (b) Channel capacity in bits per seconds versus time per channel use for Brownian motion with flow and molecular motor based active transport. ( $x_{\max} = 40$ ). Different separations between the transmitter and receiver are considered.

means of improving channel capacity of Brownian motion. Although Brownian motion itself is considered to be passive transport, Brownian motion with flow is considered to be active transport using an external device. To improve the channel capacity of molecular motor based active transport, we proposed increasing the number of microtubules as well as optimizing the shape of the transmission area using a proposed mathematical model.

Based on the obtained results, we showed that the suggested improvements increase the channel capacity of each propagation scheme significantly. We also showed that there is an optimal time duration per channel use for each propagation scheme, where information rate is maximized. Finally, we compared all propagation schemes under different separation distances between the transmitter and the receiver and showed that for the molecular communication system considered, Brownian motion with flow achieves higher information rate for smaller separation and smaller values of time per channel use, while the optimal molecular motor based active transport achieves higher rates over larger separation and larger values of time per channel use.

In this paper, the number of information particles considered was relatively small (the maximum number of particles considered was 40), because the computational complexity of our molecular motor based simulation environment increases significantly as the number of information particles increase. However, because the channel is 3-dimensional for Brownian motion and 2-dimensional for molecular motor based propagation, theoretically there could be a larger number of information particles released by the transmitter when Brownian motion or Brownian motion with flow is employed. This would result in a much higher achievable information rate for Brownian motions. However, as shown in [20], [24], it is possible to use vesicular encapsulation to incorporate a large number of information particles inside a single vesicle and mitigate this discrepancy between the Brownian motion and molecular motor based propagation schemes.

Although Brownian motion with flow seems to be slightly better than the optimized molecular motor based active transport over smaller distances, introducing flow would require an external device such as a syringe pump. Moreover, increasing the number of microtubules is very easy and can be used to increase the information rates even further. However, increasing flow is not as straightforward. Therefore, based on these results we generally believe that active transport is a better propagation scheme for on-chip molecular communication systems, which have lots of potential applications such as diagnostic chips for healthcare.

In this paper, only rectangular channels are considered. In the future we would like to consider other shapes such as a circular, elliptical and ring shaped channels. Furthermore, we would like to provide design guidelines such as optimal channel dimensions for each shape. Another direction that we would like to extend our work is optimization of our simulation environment. The number of information particles considered in this work was relatively small, because of the computational constraints of our simulation environment. Improving our simulation algorithm could help in increasing the number of

information particles.

## REFERENCES

- [1] I. F. Akyildiz, F. Brunetti, and C. Blazquez, "Nanonetworks: A new communication paradigm," *Computer Networks*, vol. 52, no. 12, pp. 2260–2279, 2008.
- [2] S. Hiyama and Y. Moritani, "Molecular communication: harnessing biochemical materials to engineer biomimetic communication systems," *Nano Communication Networks*, vol. 1, no. 1, pp. 20–30, 2010.
- [3] S. Hiyama, Y. Moritani, T. Suda, R. Egashira, A. Enomoto, M. Moore, and T. Nakano, "Molecular communication," in *Proc. of the 2005 NSTI Nanotechnology Conference*, pp. 391–394, 2005.
- [4] S. Hiyama, R. Gojo, T. Shima, S. Takeuchi, and K. Sutoh, "Biomolecular-motor-based nano- or microscale particle translocations on DNA microarrays," *Nano Letters*, vol. 9, no. 6, pp. 2407–2413, 2009.
- [5] B. Alberts, D. Bray, K. Hopkin, A. Johnson, J. Lewis, M. Raff, K. Roberts, and P. Walter, *Essential Cell Biology*. Garland, 3 ed., 2009.
- [6] T. D. Pollard, W. C. Earnshaw, and J. Lippincott-Schwartz, *Cell Biology*. Saunders, 2 ed., 2007.
- [7] T. Nakano, T. Suda, M. Moore, and R. Egashira, "Molecular communication for nanomachines using intercellular calcium signalling," in *Proc. of the 5th IEEE Conference on Nanotechnology*, pp. 478–481, 2005.
- [8] T. Nakano, T. Suda, T. Koujin, T. Haraguchi, and Y. Hiraoka, "Molecular communication through gap junction channels: System design, experiments and modeling," in *Proc. of the 2nd International Conference on Bio-Inspired Models of Network, Information, and Computing Systems*, (Budapest, Hungary), pp. 139–146, 2007.
- [9] A. Enomoto, M. Moore, T. Nakano, R. Egashira, T. Suda, A. Kayasuga, H. Kojima, H. Sakakibara, and K. Oiwa, "A molecular communication system using a network of cytoskeletal filaments," in *Proc. of the 2006 NSTI Nanotechnology Conference*, pp. 725–728, 2006.
- [10] S. Hiyama, Y. Moritani, and T. Suda, "A biochemically-engineered molecular communication system," in *Nano-Net*, vol. 3 of *Lecture Notes of the Institute for Computer Sciences, Social Informatics and Telecommunications Engineering*, pp. 85–94, Springer Berlin Heidelberg, 2009.
- [11] A. W. Eckford, "Nanoscale communication with brownian motion," in *Proc. of the 41st Annual Conference on Information Sciences and Systems*, (Baltimore, MD), pp. 160–165, 2007.
- [12] B. Atakan and O. Akan, "An information theoretical approach for molecular communication," in *Proc. of the 2nd International Conference on Bio-Inspired Models of Network, Information and Computing Systems*, (Budapest, Hungary), pp. 33–40, 2007.
- [13] A. W. Eckford, "Timing information rates for active transport molecular communication," in *Nano-Net*, vol. 20 of *Lecture Notes of the Institute for Computer Sciences, Social Informatics and Telecommunications Engineering*, pp. 24–28, Springer Berlin Heidelberg, 2009.
- [14] M. J. Moore, T. Suda, and K. Oiwa, "Molecular communication: modeling noise effects on information rate," *IEEE Transactions on NanoBioscience*, vol. 8, no. 2, pp. 169–180, 2009.
- [15] M. Pierobon and I. F. Akyildiz, "A physical end-to-end model for molecular communication in nanonetworks," *IEEE Journal on Selected Areas in Communications*, vol. 28, no. 4, pp. 602–611, 2010.
- [16] M. U. Mahfuz, D. Makrakis, and H. T. Mouftah, "On the characterization of binary concentration-encoded molecular communication in nanonetworks," *Nano Communication Networks*, vol. 1, no. 4, pp. 289–300, 2010.
- [17] A. W. Eckford, N. Farsad, S. Hiyama, and Y. Moritani, "Microchannel molecular communication with nanoscale carriers: Brownian motion versus active transport," in *Proc. of the IEEE International Conference on Nanotechnology*, (Seoul, South Korea), pp. 854 – 858, 2010.
- [18] N. Farsad, A. W. Eckford, S. Hiyama, and Y. Moritani, "Information rates of active propagation in microchannel molecular communication," in *Proc. of the 5th International ICST Conference on Bio-Inspired Models of Network, Information, and Computing Systems*, (Boston, MA), p. 7, 2010.
- [19] N. Farsad, A. W. Eckford, S. Hiyama, and Y. Moritani, "A simple mathematical model for information rate of active transport molecular communication," in *Proc. IEEE INFOCOM Workshops*, (Shanghai, P. R. China), pp. 473–478, 2011.
- [20] N. Farsad, A. W. Eckford, S. Hiyama, and Y. Moritani, "Quick system design of vesicle-based active transport molecular communication by using a simple transport model," *Nano Communication Networks*, vol. 2, no. 4, pp. 175–188, 2011.
- [21] T. Nitta, A. Tanahashi, M. Hirano, and H. Hess, "Simulating molecular shuttle movements: Towards computer-aided design of nanoscale transport systems," *Lab on a Chip*, vol. 6, no. 7, pp. 881–885, 2006.
- [22] T. Nitta, A. Tanahashi, and M. Hirano, "In silico design and testing of guiding tracks for molecular shuttles powered by kinesin motors," *Lab on a Chip*, vol. 10, no. 11, pp. 1447–1453, 2010.
- [23] N. Farsad, A. W. Eckford, and S. Hiyama, "Channel design and optimization of active transport molecular communication," in *Proc. 6th International ICST Conference on Bio-Inspired Models of Network, Information, and Computing Systems*, (York, England), 2011.
- [24] S. Hiyama, Y. Moritani, R. Gojo, S. Takeuchi, and K. Sutoh, "Biomolecular-motor-based autonomous delivery of lipid vesicles as nano- or microscale reactors on a chip," *Lab on a Chip*, vol. 10, no. 20, pp. 2741–2748, 2010.
- [25] L. C. Cobo and I. F. Akyildiz, "Bacteria-based communication in nanonetworks," *Nano Communication Networks*, vol. 1, no. 4, pp. 244–256, 2010.
- [26] T. M. Cover and J. A. Thomas, *Elements of Information Theory 2nd Edition*. Wiley-Interscience, 2 ed., 2006.
- [27] R. Blahut, "Computation of channel capacity and rate-distortion functions," *IEEE Transactions on Information Theory*, vol. 18, no. 4, pp. 460–473, 1972.
- [28] S. Arimoto, "An algorithm for computing the capacity of arbitrary discrete memoryless channels," *IEEE Transactions on Information Theory*, vol. 18, no. 1, pp. 14–20, 1972.
- [29] J. Berthier and P. Silberzan, *Microfluidics for Biotechnology, Second Edition*. Artech House, second ed., Dec. 2009.
- [30] S. X. Chen and J. S. Liu, "Statistical applications of the poisson-binomial and conditional bernoulli distributions," *Statistica Sinica*, vol. 7, pp. 875–892, 1997.